JOURNAL OF CATALYSIS 139, 611–630 (1993)

The Interaction of CO and H_2 with Bimetallic Ag/Ru(10$\bar{1}$0) Surfaces

PETRA LENZ[1] AND K. CHRISTMANN

Institut für Physikalische und Theoretische Chemie, Freie Universität Berlin, Takustr. 3, W-1000 Berlin 33, Germany

Received May 28, 1992; revised September 9, 1992

We have studied the adsorption of CO and H_2 on bimetallic Ag/Ru(10$\bar{1}$0) surfaces by means of LEED, temperature-programmed thermal desorption (TPD), and work function ($\Delta\Phi$) measurements. A systematic variation of the Ag-to-Ru surface atom ratio and the gas coverage reveals that (i) the amount of strongly chemisorbed CO or H depends on the number of adjacent (Ag-free) Ru atoms, whereby this "ensemble effect" is more pronounced for H than for CO adsorption; (ii) CO and H dipole moments as well as initial heats of adsorption decrease with increasing Ag coverage; (iii) additional (weakly bound) desorption states appear for larger CO and hydrogen exposures at lower temperatures; and (iv) the long-range order of the CO phases persists up to $\Theta_{Ag} \approx 0.5$, whereas ordered hydrogen LEED structures disappear already after $\Theta_{Ag} \geq 0.1$. The influence of Ag on the nature of the CO and H binding states and possibilities of hydrogen spillover from Ru to Ag sites are discussed in terms of geometrical and electronic interactions and compared with recent results reported for similar systems.

1. INTRODUCTION

The VIIIb group metals are generally considered catalytically very active materials. In order to optimize the activity and/or selectivity for certain reaction paths, it is attractive to modify these metals with a second (metallic) component which is often a group I (alkali or noble) metal. Interest in these bimetallic materials consisting of an (active) transition and an (inert) noble metal arose because of the peculiar activity/selectivity behavior of these systems in hydrogenation/dehydrogenation and hydrogenolysis reactions (*1–5*); a comprehensive review article by Campbell is recommended for further information (*6*). Geometrical and electronic properties were invoked to account for this behavior leading to the terms *ensemble effect* and *ligand effect* (*7*). Typical hydrocarbon reactions can be classified with regard to their site specificity: processes involving C–C bond scission (e.g., hydrogenolysis reactions) usually consist of several parallel or consecutive steps and, hence, often require specific active surface sites ("demanding" reactions). "Facile" reactions, on the other hand, such as hydrogenation, dehydrogenation, or isomerization, mostly require only one or two adjacent active sites. In order to investigate this *geometrical* effect it may be quite revealing to use the group Ib metal as a diluent which simply blocks active surface sites of the transition metal (e.g., Ru) and to probe the activity of the respective bimetallic surface as a function of the group Ib metal concentration for a given type of reaction, for example, the hydrogenolysis of alkanes. Experiments of this kind were performed for various hydrocarbon reactions on Pt/Au (*2*) and Ni/Cu surfaces (*1*, *7*, *8*).

However, besides these geometrical actions, *electronic* effects can have a great influence as well. The electronegativity of a given surface atom or ensemble of surface atoms can easily be modified by coadsorption or incorporation of chemically different atoms resulting in altered (often site-spe-

[1] Present address: Texas A&M University, Dept. of Chemistry, College Station, TX 77843-3255.

0021-9517/93 $5.00

cific, i.e., fairly localized) sticking probabilities and/or chemisorptive binding energies. Effects of this kind are quite common with the strongly electropositive alkali metals, whereas noble metals rather act via a mere site-blocking. In most cases, however, geometrical and electronic effects are difficult to delineate because of their simultaneous operation. The Cu/Pt system (*3–5*) may serve as an example here. The hydrogenolysis activity generally *increases* with copper coverage whereby the role of Cu is twofold: It promotes C–H bond scission but also acts as a hydrogen carrier via spillover. At the same time, competing hydrogenation reactions are suppressed because of Cu's site-blocking function.

Most of the aforementioned model studies were so far carried out either with polycrystalline materials or with crystallographically "smooth" low-index-single-crystal surfaces. As far as Ag-covered Ru surfaces are concerned, previous studies dealt mostly with the isotropic basal Ru(0001) plane (*9–19*). It appeared quite interesting to us to perform the respective investigations also with *anisotropic* transition metal surfaces which can provide a whole variety of different adsorption sites for both the predeposited noble metal and the post-adsorbed reactants. Furthermore, due to the surface anisotropy, direction-dependent diffusion or spillover processes are likely to occur. Accordingly, we have chosen the Ag/Ru(10$\bar{1}$0) system here, because it seemed particularly promising to us to separate electronic and geometrical effects (ligand vs ensemble effect), to scrutinize its eventual H spillover activity, and to compare the respective results with the well-known systems Au/Ru(0001) (*14, 15*) Cu/Ru(0001) (*16–21*), and Ag/Ru(0001) (*10–12*). A separate report will be published about the interaction of silver with a Ru(10$\bar{1}$0) surface (*22*).

From previous studies (*10, 11*) it is well established that Ag and Ru are neither miscible in the bulk nor in the surface, and Ag/Ru bimetallic surfaces with well-defined chemical composition and structure can easily be prepared. As regards our choice of the two probe gases CO and H_2, we recall that these molecules are the essential reactants in the Fischer–Tropsch reaction. Furthermore, they differ substantially in their adsorptive behavior: CO adsorbs molecularly and favors (at least on Ru) sites with a low coordination (*23*), whereas hydrogen adsorbs dissociatively on Ru and rather prefers highly coordinated sites (*24*). Marked differences exist also with respect to the CO–Ru and H–Ru binding energies: Previous studies showed that CO adsorbs quite strongly on pure Ru(10$\bar{1}$0) (*25*) leading to pronounced binding states between 330 and 530 K. On Ag, CO adsorption is usually very weak, the heats of adsorption being less than 40 kJ/mole (*26*). At 80 K the molecular adsorption of H_2 on Ag is not possible (*27, 28*), whereas previous measurements revealed that H_2 adsorbs easily on Ru(10$\bar{1}$0) (*24, 29, 30*).

2. EXPERIMENTAL

The experiments were performed in an all-stainless-steel UHV chamber equipped with a 4-grid LEED optics, a cylindrical mirror analyzer (CMA) with integral electron gun for Auger electron spectroscopy (AES), a quadrupol mass spectrometer for the TPD experiments, a Kelvin probe for $\Delta\Phi$ measurements, and a vibrational loss (HREELS) electron spectrometer. More details about the experimental techniques and their modes of operation, as well as about sample handling, preparation, and cleaning, can be found elsewhere (*24, 25*). Silver layers of desired thicknesses were prepared using an electronically regulated Ag evaporation source (*31*); the Ru surface was kept at a temperature of 735 K during Ag deposition. The Ag coverages were determined by taking the Ag TPD-peak integrals as well as from Auger electron spectra as described in more detail elsewhere (*22*). Thereafter either the adsorption of CO or that of hydrogen was studied, whereby the sample temperature was sufficiently lowered ($T_{ad} \approx 80$ K) and the gas exposures

increased (≤50 L) in order to populate *all available adsorbate binding states* including *chemisorbed and* weakly held species, in agreement with our previous studies (*24, 25*). However, in our measurements of the ensemble requirements for chemisorption, we had to ensure that *only the chemisorbed states* became filled. Limitation of the hydrogen gas exposure to only 10 L (instead of saturation exposure) ruled out the influence of the weakly held adsorbate species which is likely to adsorb in Ag-like sites via *spillover* (cf., Section 4.2); similarly, by choosing T_{ad} = 300 K and only a 10-L exposure during CO adsorption, we could separate strongly chemisorbed from more weakly adsorbed CO.

3. RESULTS

3.1. Ag on Ru(10$\bar{1}$0)

(Video)-LEED, AES, TPD, ΔΦ measurements, and CO-adsorption at 300 K were utilized to characterize the growth and structure of the Ag overlayers. While a comprehensive report is given elsewhere (*22*) we present only a brief summary here. Since CO does not adsorb on Ag at 300 K but easily does so on Ru, we could "titrate" the Ru surface atoms not covered by Ag by means of CO. The respective measurements revealed a clear island-growth mode of Ag up to a coverage of Θ_{Ag} = 0.6; interestingly, a silver-induced c(2×2) LEED pattern appeared even at the smallest Ag coverages indicative of attractive Ag–Ag interactions and the formation of islands. A brief comment concerning the definition of the coverage Θ may be useful here: We understand Θ as a dimensionless fraction of the total number of silver atoms adsorbed *on top of the Ru surface* related to the number of *topmost Ru surface atoms* (= 8.638 × 10^{14} cm^{-2} for the (10$\bar{1}$0) orientation). As pointed out elsewhere (*22*), a structural model for the Ag c(2×2) can be deduced which demands a *homogeneous* Ag coverage of $\frac{3}{4}$. However, if we take the desorption peak integral $\int p_{Ag}dt$ as a measure of the coverage in the above sense, we overestimate the actual *surface* coverage because of the pronounced island growth and early 3D-clustering of Ag—actually, at the c(2×2) LEED intensity maximum the surface is covered only by ≈80% of the nominal coverage of 0.75. Therefore, the *effective* silver coverage $\Theta_{Ag,eff}$ rather is ~0.6 instead of 0.75.—In the thermal desorption experiments, we find, below $\Theta_{Ag} \sim 0.6$, only a single (β_2)-state due to chemisorbed silver. In AES, a plot of the signal ratio (Ag(351 eV)/Ru(321 eV)) versus silver coverage also reveals a break around $\Theta_{Ag} \approx 0.6$. Likewise at this coverage, a second (β_1) desorption state grows in on the low-temperature tail of the β_2-state, and new LEED structures ((10 × 1) and c(14 × 5)) become visible in addition to the still persisting c(2×2) structure. These features indicate the sudden onset of three-dimensional Ag growth around $\Theta_{Ag} \approx$ 0.6, whereby however, as the CO titration measurements show, there remain even at $\Theta_{Ag} \approx$ 5 still some uncovered Ru sites left. The reason for this behavior must be sought in a strong attractive interaction between the Ag atoms leading to pronounced island growth (which was reported previously (*32, 33*)). This, in turn, is responsible for a reduced mobility of those Ag atoms or nuclei formed on top of a two-dimensional Ag island. At a certain critical diameter of such an island the three-dimensional growth is energetically more favorable, resulting in a modified Frank–van der Merwe growth mode, the so-called Simultaneous Multilayer (SM) growth (*34, 35*).

3.2. Adsorption of CO on Ag/Ru

3.2.1. LEED measurements. On pure Ru(10$\bar{1}$0) CO adsorption at 100 K gives rise to the formation of six different ordered phases (*25*), namely, a (3 × 1) at Θ_{CO} = 0.3; a c(2 × 8) at Θ_{CO} = 0.45, a np(3 × 1) at Θ_{CO} = 0.67, a (4 × 1) at Θ_{CO} = 0.75, a np(2 × 1) at Θ_{CO} = 1.0, and a $\begin{pmatrix} 4 & \frac{1}{2} \\ 1 & \end{pmatrix}$ structure at Θ_{CO} = 1.22. At sufficiently low adsorption temperatures and small Ag precoverages ($\Theta_{Ag} \leq 0.4$), all these LEED phases could be observed also in the presence of silver,

whereby increasing Θ_{Ag} caused, however, increasing background intensity due to partial random disorder. No *additional* CO structures could be observed, even not with a filled γ_1-state. As the CO-covered Ru/Ag surfaces are gently heated to ~200 K, the first three ordered phases disappear, while the np(2 × 1) is stable up to 250 K. Interestingly, the complex compression structure remains visible even at room temperature, a behavior that was observed also with the clean CO/Ru(10$\bar{1}$0) system. It was particularly interesting to investigate the coexistence of the Ag-induced c(2 × 2) and the CO-induced compression structure; actually this CO structure could be observed up to $\Theta_{Ag} = 0.48$, where the Ag-c(2 × 2) LEED pattern is already very well developed. In principle, one could argue that the CO adsorbs in empty Ru sites *within* the c(2 × 2) unit cell; however, this would correspond to kind of a cooperative adsorption and should lead to a superposition of scattering contributions *within* an Ag c(2 × 2) unit cell and, hence, alter the scattering amplitudes resulting in new LEED features which are *not* observed. Instead, we find coexistence of both spot systems, indicating a superposition of individual scattering intensities. This is compatible with the formation of separate Ag and CO-on-Ru islands whose diameter is larger than the coherence width of the LEED beam, i.e., > 100 . . . 200 Å. This is strong evidence for silver clustering in islands as pointed out before, whereby at least at *room temperature* the CO only adsorbs on those Ru patches which are not or only little influenced by Ag.

3.2.2. Temperature-programmed desorption spectroscopy. Both the clean and the partially Ag-covered ($\Theta_{AG} \approx 0.49$) Ru(10$\bar{1}$0) surface were exposed at $T_{ad} = 300$ K to increasing amounts of CO (exposure in [L]; 1 [L] = 1.332×10^{-4}[Pa s]) and then linearly heated with a rate β of 10 K s^{-1}. Figures 1a and 1b show the corresponding series of TPD spectra for the pure Ru(10$\bar{1}$0) (a) and the bimetallic Ag/Ru(10$\bar{1}$0) surface (b). Apparently, the CO TPD spectra obtained from the bimetallic surface are quite similar to those from the clean Ru(10$\bar{1}$0) surface. All desorption states characteristic for clean Ru(10$\bar{1}$0), namely, a first-order β_3-state with T_{max} between 500 and 520 K, a β_2-peak around 400 K, and a β_1-state at 380 K (*25*), can also be distinguished in the Ag/Ru(10$\bar{1}$0) surface spectra. It is noteworthy that there is no specific CO TPD state due to the bimetallic surface under these conditions. The only difference consists in a slight shift of the desorption maximum and the relative intensity of the β_3-state: As compared with the β_2- and β_1-states, β_3 is relatively more suppressed for the bimetallic surfaces (actually, the respective loss of intensity increases with Θ_{Ag}); furthermore, we observe a shift of the β_3 desorption temperature maximum from ~520 K to ~480 K.—However, if we adsorb CO at 100 K instead of 300 K, an additional CO TPD peak characteristic of the bimetallic surface, the γ-state, grows in at temperatures between 340 and 380 K; its intensity as well as its maximum position depends strongly on the CO exposure. Figure 2 shows an example for $\Theta_{Ag} = 0.4$. Interestingly, the γ-maximum is, within certain limits, *independent* of the Ag precoverage, at least up to $\Theta_{Ag} \approx 0.6$, that is, as long as there occurs predominantly two-dimensional growth. Also quite remarkable is that the γ-state could never be observed in our room temperature adsorption measurements, although its maximum temperature appears ~60 K above room temperature. Apparently, the sticking probability into this γ-state is strongly temperature-dependent and does not allow its population at 300 K.—All other TPD states described above for the room temperature adsorption persist and do not exhibit noticeable changes, neither in their peak temperature position nor in intensity. For higher silver coverages and saturation CO exposures, however, the γ intensity gradually decreases and disappears around $\Theta_{Ag} = 1.5$, whereby at this high Ag coverage all CO TD states are blurred and no longer really distinguishable.

In order to quantify the influence of the

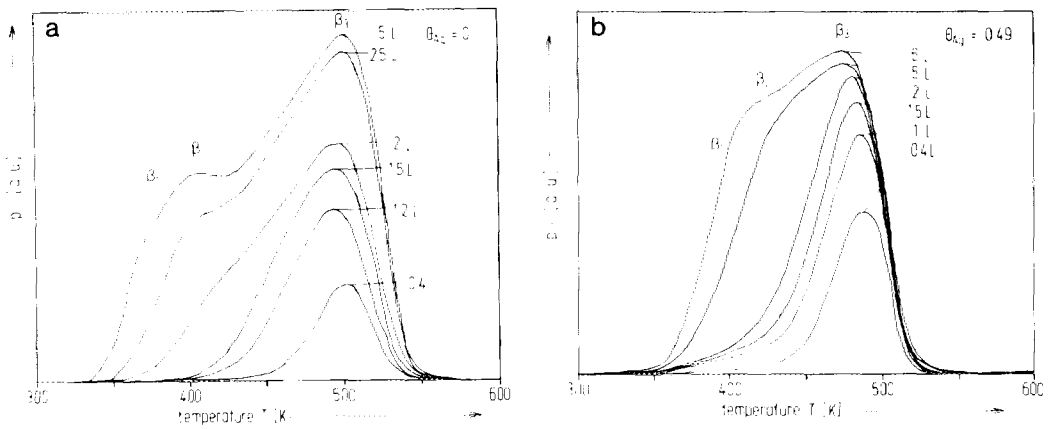

FIG. 1. Series of thermal desorption spectra of CO from clean Ru(10$\bar{1}$0) (a) and from a bimetallic Ag/Ru surface (Θ_{Ag} = 0.49) (b) after increasing exposures (0.4, ..., 6 L) at T_{ad} = 300 K. The heating rate was always β = 10 K s^{-1}. The CO partial pressure scale is blown up in (b).

silver on the CO adsorption we have performed desorption experiments where bimetallic surfaces with increasing silver surface concentration ($0.07 \leq \Theta_{Ag} \leq 0.95$) were exposed to a constant dose of 10 L CO. The result is shown in Fig. 3a and confirms the statement made before, whereafter the β_3 CO TPD-state is more affected by Ag than the β_2- and β_1- states. We have also extended these 10-L CO adsorption experiments up to a silver precoverage of five nominal layers. We recall that a CO exposure of 10 L on clean Ru(10$\bar{1}$0) was more than sufficient to fill all CO chemisorption states; in case of the bimetallic surfaces at least all strongly bound CO species should be included. (In order to also map the weakly held CO the respective *saturation* exposure would have to be applied). Accordingly, the respective CO-TPD spectra from the bimetallic surfaces then reveal another valuable information, namely, the total *uptake* of strongly held CO as a function of Θ_{Ag}: In Fig. 3b we have plotted the total area $\int p_{CO} dt$ under a CO-TPD curve against Θ_{Ag}, and the respective graph shows quite clearly a relatively strong suppression of the amount of adsorbed CO with increasing silver coverage as long as $\Theta_{Ag} < 1$. As mentioned in the beginning, there is then only a slight decrease of $\int p_{CO} dt$ in the range $2 \leq \Theta_{Ag} \leq 5$, thus pointing to a relatively constant number of still accessible Ru surface atoms in this coverage regime and indicating certain "holes" in the silver film on top of the Ru surface. It is essential in these experiments to carefully consider eventual desorptive contributions from sample holder and crystal edges. We have, therefore, performed

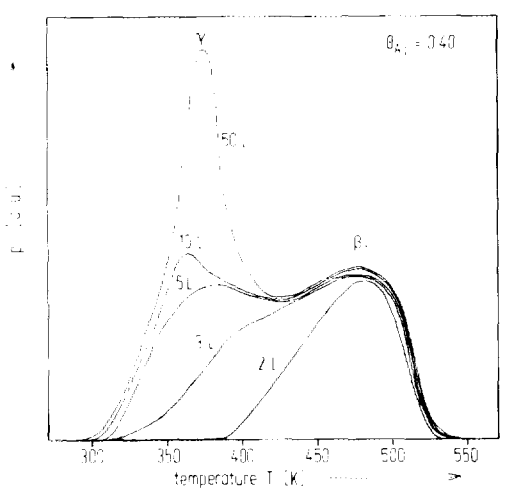

FIG. 2. Thermal desorption spectrum of CO from Ag/Ru (Θ_{Ag} = 0.40) after CO exposures up to 50 L at 100 K. Note the appearance of a new γ-state around ~370 K for exposures greater than 3 L.

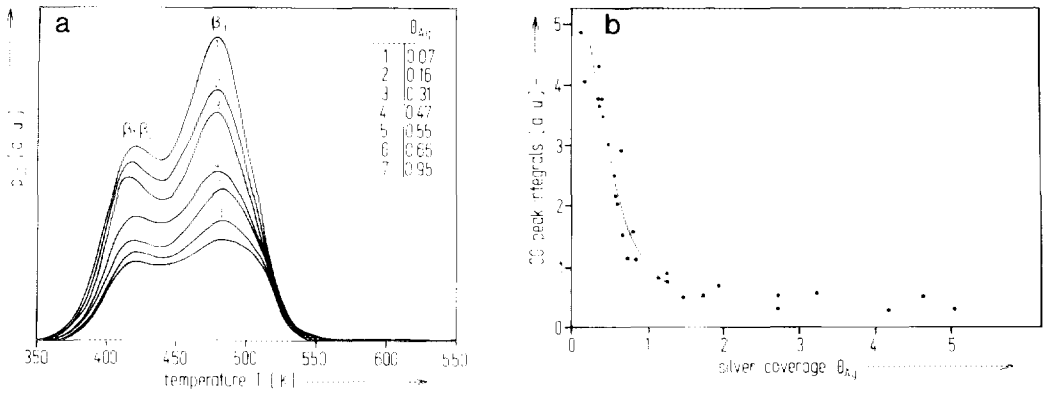

FIG. 3. (a) Series of CO thermal desorption spectra from bimetallic Ag/Ru surfaces ($0.07 < \Theta_{Ag} < 0.95$) after a constant exposure of 10 L at 300 K. (b) Plot of the 10 L CO uptake $\int p_{CO} dt$ after room temperature adsorption (as determined from TPD spectra) as a function of the silver coverage (Θ_{Ag}).

blank experiments with a completely carbon (sulfur) contaminated sample which revealed absolutely *no* CO or hydrogen uptake. Since the sputter-cleaning only affects the front face of the Ru crystal, we consider the aforementioned gas uptake at elevated Ag coverages not as an artifact.

A problem encountered at this part of our work is the determination of absolute adsorbate (CO, H) coverages. The Θ_{CO}-calibration is closely tied to the absolute CO coverage of the bare Ru(10$\bar{1}$0) surface, where Θ_{max} was found to be 1.22 giving rise to a $\begin{pmatrix} 4 & -\frac{1}{2} \\ 1 & \end{pmatrix}$ compression structure; the clear (2 × 1)p2mg LEED structure which occurs at somewhat lower coverages could be unequivocally associated with $\Theta_{CO} = 1$ (*25*). Since we find, for $T_{ad} = 300$ K, all characteristic CO surface binding states also on the bimetallic surfaces (at least up to $\Theta_{Ag} = 0.5$), we may define a *local* CO coverage which refers to CO adsorbed on the *uncovered* (i.e., Ag-free) Ru surface patches. This *local* CO coverage then is (within certain limits) *independent* of the silver coverage, whereas the *overall* CO coverage (related to the entire bimetallic surface), does, of course, depend on the Ag coverage, and Θ_{Ag} must be known in order to deduce the overall absolute CO coverage from the known local CO coverage. Somewhat more difficult is the situation at $T_{ad} = 100$ K, where the additional CO γ-state comes into play which likely reflects CO bound in low-energy surface sites that are only present at higher Ag surface concentrations.

Finally, one can determine effective activation energies for CO desorption from the bimetallic Ag/Ru surfaces and compare them with those obtained from bare Ru(10$\bar{1}$0). For the respective evaluation, we have chosen the lineshape analysis as proposed by King (*36*) which does not a priori assume coverage-independent activation energies or frequency factors. We present, in Fig. 4, as an example, the coverage dependence of the CO activation energy for desorption, based on our TPD data measured at $\Theta_{Ag} = 0.4$, along with the respective data for the Ag-free Ru(10$\bar{1}$0) surface. At small CO coverages ΔE^*_{CO} (which equals, for this case of nonactivated molecular desorption, the CO-substrate binding energy) tends toward 110 kJ/mol, but increases with $\Theta_{CO,loc}$ by some 10 kJ/mol until the β_3-state is filled around $\Theta_{CO} \approx 0.3$, before it drops continuously to a level of ~90 kJ/mol at CO saturation. A comparison with the "bare" Ru/CO data (open circles) reveals a relatively similar curve shape, whereby, however, the energies of the "bare" system generally exceed those of the bimetallic

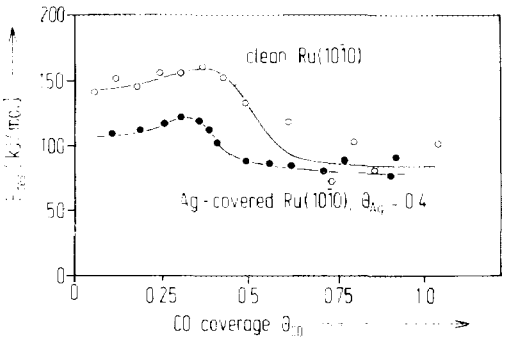

FIG. 4. Coverage dependence of the activation energy for desorption of CO from a bimetallic Ag/Ru(10$\bar{1}$0) surface containing $\Theta_{Ag} = 0.40$ (dark circles), and from clean Ru(10$\bar{1}$0) (open circles), as determined from a lineshape analysis after King (*36*).

system by ~40 kJ/mol. Also, the maximum in the adsorption energy associated with the saturation of the β_3-state is somewhat shifted to higher CO coverages. Turning to the overall Θ_{Ag} effect, we encounter even at the smallest silver precoverages a relatively marked decrease of the CO adsorption energy, which we found already with the $\Theta_{Ag} = 0.4$ example above. Higher Θ_{Ag} precoverages show this effect even more distinctly; at $\Theta_{Ag} \approx 0.95$ the CO adsorption energy at saturation amounts to merely 80 kJ/mol. The desorption energy of the γ-state (whose maximum does not shift with the CO coverage) can be estimated on the basis of the simple first-order analysis according to Redhead (*37*) using the formula

$$E^*_{des} = RT_{max}\left(\frac{\nu T_{max}}{\beta} - 3.64\right), \qquad (1)$$

with: ν = frequency factor (usually taken as 10^{13} s^{-1}) and $\beta = dT/dt$ = heating rate (≈10 K/s in this case).

We thus determine the activation energy for CO desorption from the γ-state to be less than 90 kJ/mol, a value which is considerably smaller than the usual CO chemisorption energies of ~130 kJ/mol.

As another point of interest, we briefly consider the CO adsorption *kinetics* which was followed by TPD (and $\Delta\Phi$) measurements. While *absolute* sticking probabilities are difficult to determine with sufficient accuracy, *relative* quantities are more easily evaluated simply by comparing the TPD peak area $\int p_{CO} dt$ for given CO exposures with the saturation spectrum. In Fig. 5 we present two examples for the coverage dependence of the relative sticking probability s/s_0 taken for $\Theta_{Ag} = 0.18$ and $T_{ad} = 300$ K (Fig. 5a) and for $\Theta_{Ag} = 0.32$ and $T_{ad} = 100$ K (Fig. 5b). In both cases we find a practically constant sticking coefficient up to a CO coverage of ~0.8 . . . 0.9, quite comparable to the clean Ru(10$\bar{1}$0) surface (*25*), with a strong decrease to zero at $\Theta_{CO} = 1.2$ for the room-temperature adsorption and a much more gradual decay to zero at $\Theta_{CO} \approx 1.5$ for the low-temperature adsorption case, caused by the additional population of the γ-state. An estimation of the *absolute* sticking probability based on our CO coverage calibration reveals that s_0 is very likely close to unity, as with the clean Ru surface. All in all, the coverage dependence of s on the bimetallic surfaces resembles very much that of the Ag-free Ru(10$\bar{1}$0) surface; the constant initial sticking coefficient points to a pronounced precursor state adsorption kinetics (*38*), which apparently is hardly affected by the presence of the silver at least as long as there are "free" Ru patches accessible.

3.2.3. Work function ($\Delta\Phi$) *measurements.* CO adsorption on clean Ru(10$\bar{1}$0) at 100 K leads to a monotonous work function increase of ~1130 meV at saturation, where all β adsorption states are filled (*25*). In the presence of silver we expect a somewhat different $\Delta\Phi$ behavior due to (i) changes in the amount of adsorbed CO and (ii) alterations of the Ru electronic band structure induced by Ag which may affect the CO binding mechanism to some extent. This, in turn, could be reflected as changes of the CO-Ru dipole moment. The existence of the γ-state at low enough adsorption temperatures could be taken as a hint to such a differently bonded CO species. In Fig. 6a we display, for a variety of Ag precover-

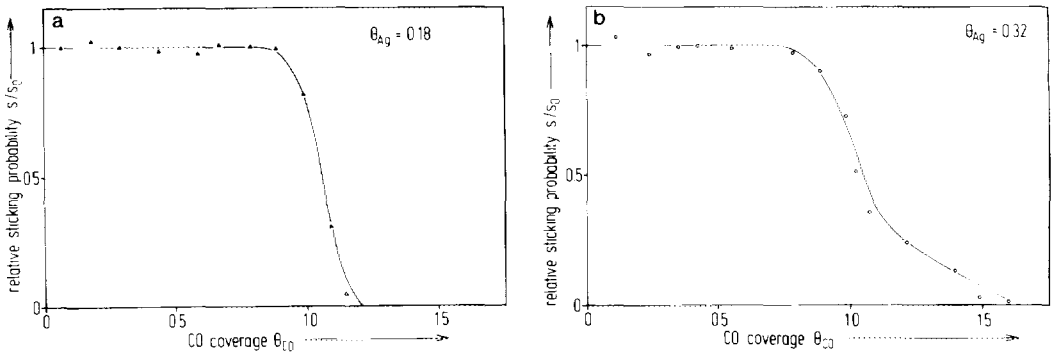

FIG. 5. Coverage dependence of the relative sticking probability $s' = s/s_0$ for CO on bimetallic Ag/Ru surfaces: (a) Silver coverage $\Theta_{Ag} = 0.18$, adsorption temperature 300 K. (b) Silver coverage $\Theta_{Ag} = 0.32$, adsorption temperature 100 K.

ages, the exposure dependence of the CO-induced work function change. Quite clearly, the $\Delta\Phi$ saturation values decrease in proportion to Θ_{Ag}. At $\Theta_{Ag} = 0.56$, for example, $\Delta\Phi$ amounts to merely 200 meV. The results of various experiments are compiled in Fig. 6b which reveals an almost linear relationship between the $\Delta\Phi$-drop and Θ_{Ag}. In order to determine the CO dipole moments we must first consider how much the CO uptake is reduced by Ag; this information can easily be obtained from TPD measurements; cf. Fig. 2. Accordingly, we have, in Fig. 7, plotted the CO-induced $\Delta\Phi$ versus the effective CO coverage for two different silver coverages, viz., $\Theta_{AG} = 0.08$ and 0.22, along with the data for clean Ru. If we take the initial slope as a measure for the initial dipole moment μ_0 and neglect depolarization effects, we can easily deduce values for μ_0 according to the simple Helmholtz equation,

$$\mu_0 = \frac{\Delta\Phi}{f^* 4\pi\Theta\sigma_{max}}, \qquad (2)$$

with $f^* = 1/4\pi\varepsilon_0$ (ε_0 = vacuum permittivity), and σ_{max} = dipoles/unit area.

While for clean Ru(10$\bar{1}$0) μ_0 is ~0.34 Debye (1 [D] = 3.33 = 10^{-30} [As]), we have for $\Theta_{Ag} = 0.08$ a μ_0 of 0.22, for $\Theta_{Ag} = 0.22$

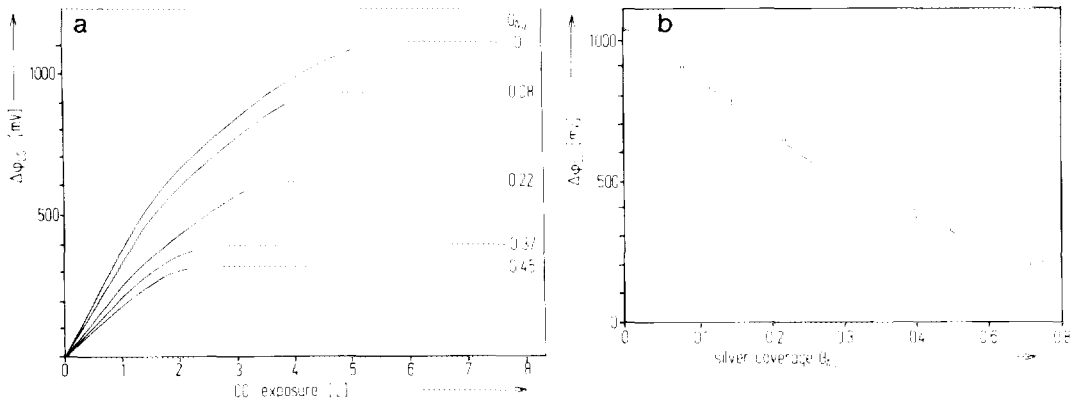

FIG. 6. Exposure dependence of the work function change due to CO at 300 K. (a) Compilation for various Ag coverages ($0 < \Theta_{Ag} < 0.45$). (b) Plot of the saturation value $\Delta\Phi_{max}$ against the silver coverage.

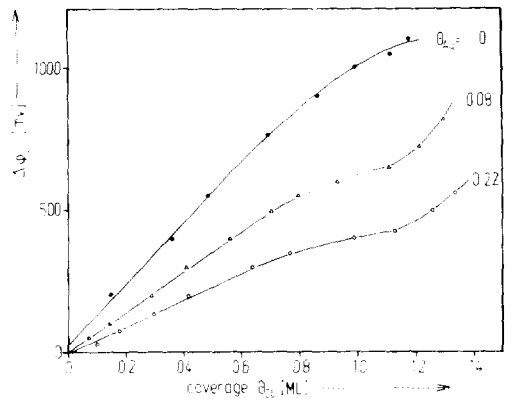

FIG. 7. CO-induced work function change $\Delta\Phi$ as a function of CO coverage, for clean Ru(10$\bar{1}$0) and Θ_{Ag} = 0.08 and 0.22 at T = 300 K.

a μ_0 of 0.14, and for Θ_{Ag} = 0.45 a μ_0 of 0.12, which means a reduction of the Ag-free value by almost two-thirds. This net loss of μ_0 could either come about by a mixing-in of adsorbate complexes with a different (low) constant dipole moment μ_0' to dipoles with unchanged μ_0 or by a general overall decrease of all dipole moments (μ_0''). Unfortunately, we cannot distinguish between these possibilities, because the $\Delta\Phi$ measurement (performed via the Kelvin vibrating capacitor method) integrates and averages over all dipole moments present on the surface at a given CO coverage. Nevertheless it is safe to assume that with increasing Θ_{Ag} more CO dipole moments become reduced, owing to a specific electronic interaction between Ag and Ru. This interaction could either lead to a modification of existing Ru-like sites and/or to the generation of new sites (with a more Ag-like character) on which the CO binding (as described by the well-known Blyholder chemisorption model (*39*)) occurs with a smaller electron backdonation thus reducing the net dipole moment. This latter explanation is perhaps corroborated by the observation of the TPD γ-state mentioned before, but a final decision here would require UV photoemission measurements in order to map the possibly different CO orbital energies. As will be shown next, even HREELS experiments are unable to clearly delineate different CO species (or CO adsorption sites).

3.2.4. High-resolution electron energy loss spectroscopy (HREELS). HREEL spectra of adsorbed carbon monoxide were recorded at 100 K for different Ag precoverages; the scattering geometry was chosen so as to probe preferentially dipole scattering (specular geometry). In a previous publication (*25*) we determined the CO-induced vibrational losses as ν_{Ru-CO} = 440 cm^{-1}, ν_{C-O} at 2000 cm^{-1} (on-top coordination), and ν_{C-O} = 1810 cm^{-1} (higher coordination at elevated coverages). On the bimetallic surfaces we observed practically the same loss frequencies and also a similar CO coverage dependence, namely, a slight red shift of the Ru–CO vibration ($\Delta\nu \approx -15$–20 cm^{-1}) and a somewhat larger blue shift of ν_{C-O} ($\Delta\nu \approx$ 60–70 cm^{-1}) as Θ_{CO} saturates. In Fig. 8a we reproduce a set of typical loss spectra for Θ_{Ag} = 0.17, obtained after three different CO exposures. Furthermore, we realize the complete *absence* of additional CO losses due to silver, even under conditions where the new γ thermal desorption state appears (cf., Fig. 2). As far as the influence of the silver precoverage is concerned we find, according to Fig. 8b, a significant red shift of ν_{Ru-CO} ($\Delta\nu \approx -70$ cm^{-1}) and a (somewhat smaller) blue shift of ν_{C-O} ($\Delta\nu_{C-O} \approx 25$ cm^{-1}), indicating some influence of the Ag on the binding force constants. Within the limits of accuracy we do not observe any substantial loss peak broadening, which could point to the occupation of energetically inhomogeneous adsorption sites as provided by differently Ag-covered or coordinated ruthenium atoms in the presence of silver.

3.3. Adsorption of hydrogen on Ag/Ru

3.3.1. LEED measurements. The interaction of hydrogen with pure Ru(10$\bar{1}$0) was studied extensively in the past (*24*), and it is well established that H_2 adsorbs *dissociatively* without noticeable activation barrier in several different binding states. A variety of ordered H LEED phases were observed:

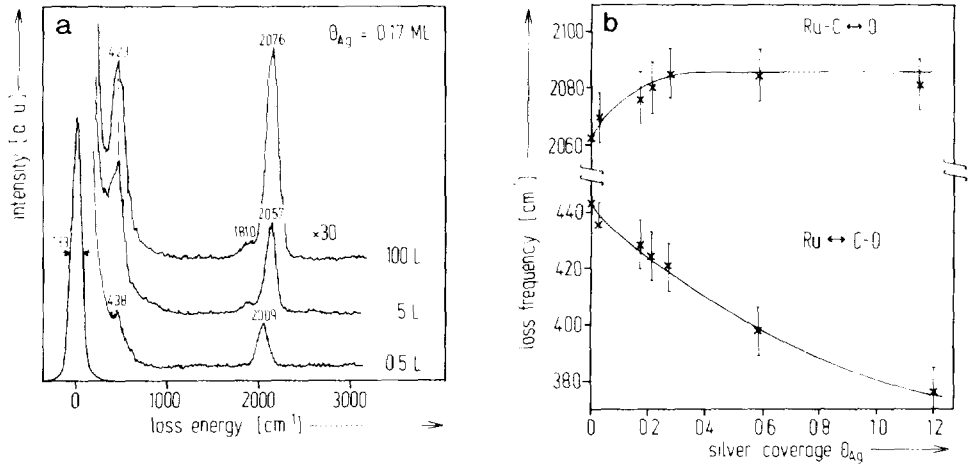

FIG. 8. HREEL spectra for CO on Ag/Ru (Θ_{Ag} = 0.17) for three different CO exposures at T_{ad} = 100 K: 0.5 L, 5 L, 100 L. (b) Frequency shifts of the ν_{C-O} and ν_{Me-CO}-bands as a function of the silver precoverage ($0 < \Theta_{Ag} < 1.2$); T_{ad} = 100 K. In all measurements CO was exposed to saturation.

A dim c(8 × 2) structure around Θ_H = 1 was followed by a (1 × 2) phase ($\Theta_H \approx 1.2$) and a relatively intense c(2 × 2) structure at Θ_H = 1.5, before all "extra" spots disappeared as the coverage approached Θ_H = 2. Low temperatures ($T_{ad} \leq 150$ K) are required to establish the long-range order within the H phases; even small amounts of contaminants suppress the order completely. In contrast to CO adsorption, where the presence of silver atoms up to $\Theta_{Ag} \approx 0.5$ did not affect the long-range order vigorously, even tiny amounts of Ag make all H-induced "extra" spots disappear, although the H atoms are still present on the surface as deduced from TPD measurements. Whether or not this structural change is accompanied by an increase of the diffuse background intensity due to disordered hydrogen cannot be said with certainty, because the partially disordered silver atoms themselves contribute already to the diffuse background and hydrogen is a very weak electron scatterer.

3.3.2. Temperature-programmed desorption spectroscopy. The clean and the partially Ag-covered Ru(10$\bar{1}$0) surfaces were exposed to hydrogen at T_{ad} = 80 K, because it was found in a previous study (*24*) that hydrogen saturation (i.e., Θ_H = 2) requires fairly low adsorption temperatures. The results are compiled in Figs. 9a (clean surface) and 9b (bimetallic surface, Θ_{Ag} = 0.49). All four TPD states (α, β_1 – β_3) observed with clean Ru(10$\bar{1}$0) are also seen with the bimetallic surface. Similar to CO desorption (cf., sect. 3.2.2) it is the high-temperature β_3-state that loses intensity relative to all other states. Up to $\Theta_{Ag} \leq 0.5$, no additional hydrogen-induced TPD maxima appear in the spectra; however, for $\Theta_{Ag} \geq 0.5$ and large H_2 exposures at 80 K (30 L and more) two *additional* hydrogen desorption states denoated as γ_1 and γ_2 develop on the low-temperature tail of the α-state at 139 and 170 K. This is illustrated in Fig. 10 for Θ_{Ag} = 0.60. Up to Θ_{Ag} = 0.80 we find increasing population of the γ-states; still higher precoverages degrade the amount of γ-hydrogen, until at $\Theta_{Ag} > 1$ it disappears completely. We note that the intensity especially of the γ_1-state depends strongly on the degree of lateral dispersion of the silver: γ_1 is small, if hydrogen is adsorbed on bimetallic surfaces partially covered with well-ordered Ag islands (careful annealing after deposition of Ag → intense c(2 × 2) LEED pattern), but it is quite large, if H_2 is exposed to

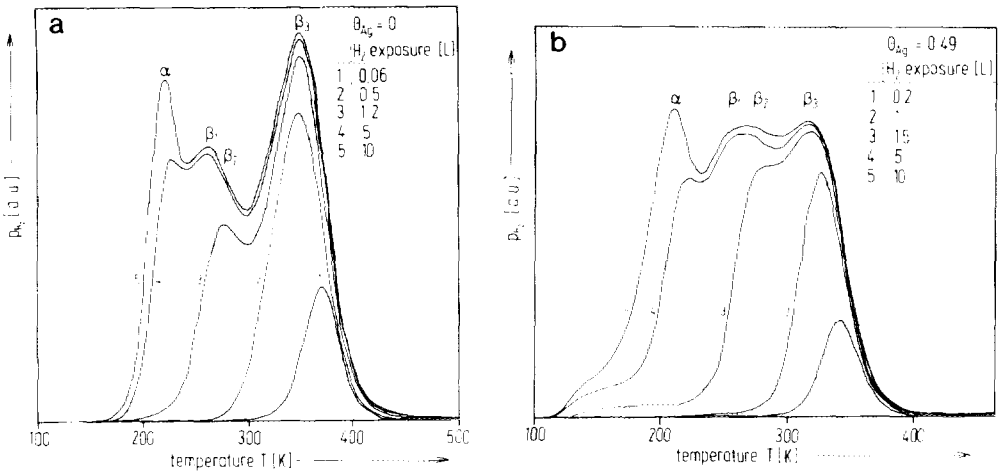

FIG. 9. Hydrogen thermal desorption spectra obtained from clean (a) and Ag-covered Ru(10$\bar{1}$0). Θ_{Ag} = 0.49 (b) after increasing H_2 exposures at 100 K ranging from 0.06 to ~10 L.

Ru surfaces which are rather covered with largely dispersed Ag atoms or small nuclei (Ag deposition at 80 K without annealing → very dim c(2 × 2) + intense LEED background). This behavior suggests that the γ-states are dominated by silver-like sites. We have performed H_2 adsorption experiments, where we exposed bimetallic surfaces ($0.12 < \Theta_{Ag} < 1.1$) to the constant hydrogen dose of 10 L and took TPD spectra in order to compare the intensity and desorption maxima as a function of the Ag coverage. We recall that—similar to the CO case—with clean Ru(10$\bar{1}$0) 10 L H_2 was more than sufficient to saturate all H binding states; on the bimetallic surfaces, as pointed out before, 10 L is sufficient to fill just all α- and β-states, but not to also populate the (very weakly held) γ-states, which are apparently characterized by an extremely low sticking probability. Hence, the exposure of 10 L is suited to delineate strongly and weakly adsorbed hydrogen, which is important in the context of the ensemble size determination discussed later. The corresponding experimental desorption spectra are reproduced in Fig. 11a and show two effects quite clearly: (i) All TPD states shift to lower temperatures ($\Delta T \approx 40$–50 K) and (ii) the peak separation becomes increasingly worse as Θ_{Ag} increases; at $\Theta_{Ag} = 1.1$ there remains only a single extremely broad desorption feature pointing to a strong energetic heterogeneity of the hydrogen adsorption sites. We have integrated the total area of these spectra and plotted it as a function of the silver coverage; the result is shown in Fig. 11b. Somewhat similar to the CO case (cf., Fig. 3b), we find a strong initial decrease

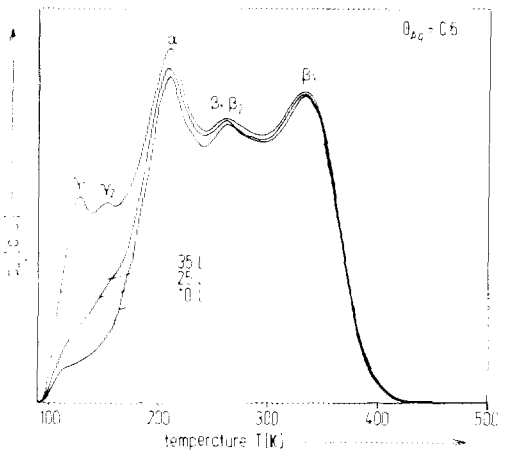

FIG. 10. Hydrogen desorption spectra taken from Ag/Ru (Θ_{Ag} = 0.60) after exposure at 100 K to 10, 25, and 35 L H_2 gas. Note the occurrence of the two γ-states!

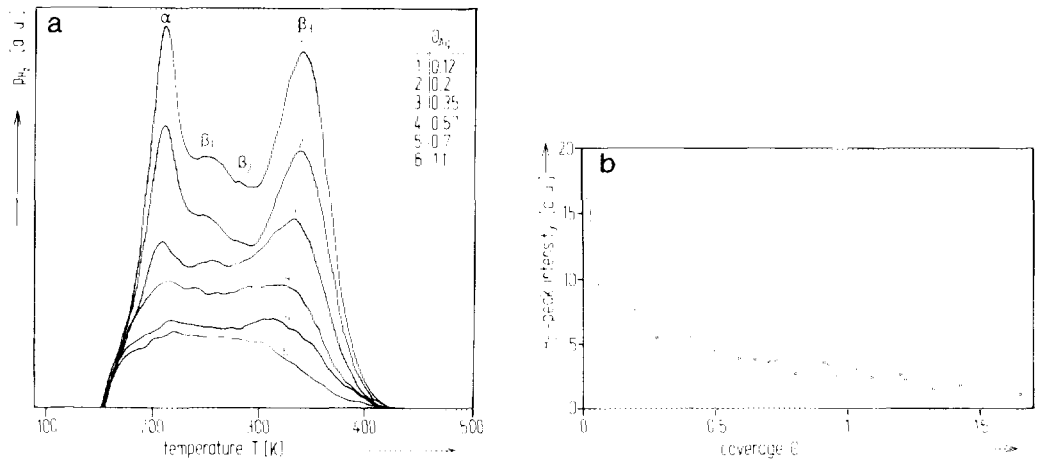

FIG. 11. (a) Hydrogen thermal desorption spectra obtained from various bimetallic Ag/Ru surfaces ($0.12 < \Theta_{Ag} < 1.1$), after a constant exposure of 10 L at $T_{ad} = 100$ K. (b) Total hydrogen uptake (as determined by integration $\int p_H dt$ of the spectra of (a) versus the silver coverage Θ_{Ag}.

between $0 < \Theta_{Ag} < 0.2$ and a much shallower decay for $\Theta_{Ag} > 0.5$; again, even at $\Theta_{Ag} = 1.5$ there is still a nonnegligible H adsorption capacity which points to the aforementioned "hole" structure of the silver film on top of the Ru surface. In contrast to the CO adsorption, however, this additional adsorption capacity is relatively small. One can argue that the bare Ru islands must be somewhat larger than in the CO case in order to bond H atoms with sufficient adsorption energy.

If we attempt to evaluate *absolute* hydrogen coverages we may proceed in a similar manner as we did with the CO coverage calibration. On clean Ru(10$\bar{1}$0) the well-developed c(2 × 2) LEED pattern could be associated with $\Theta_H = 1.5$; under these conditions, the β_1-state was approximately filled, while the completion of the α-state paralleled the saturation of the surface with hydrogen, i.e., indicated $\Theta_H = 2$ (*24*). Unfortunately, we can no longer observe H LEED patterns in the presence of Ag; this makes a determination of absolute H coverages difficult and inaccurate—the only means to judge the (local) coverage is to carefully consider the appearance of the various H TPD states and correlate their intensity with the respective surface concentration.

Concerning the activation energies for hydrogen desorption from the bimetallic surfaces we note that the TPD maxima are, if at all, only slightly shifted to lower temperatures compared with the clean Ru(10$\bar{1}$0) case, whereby the largest effect is observed with the high-temperature β_3-state. Again, we have subjected the series of TPD spectra to a lineshape analysis; however, this method is unable to give reliable results for any other than the β_3-state because of the significant overlap of the other maxima. The result for β_3 is illustrated by Fig. 12 which shows the coverage dependence of the activation energy for H_2 desorption determined for a bimetallic surface with $\Theta_{Ag} = 0.2$. We evaluate an initial energy of ~73 kJ/mol which drops to ~50 kJ/mol around $\Theta_H = 0.5$. A similar behavior was found with the bare Ru(10$\bar{1}$0) surface (*24*); the respective $E^*_{des}(\Theta_H)$ function is also marked in Fig. 12. For this example of $\Theta_{Ag} = 0.2$, E^*_{des} is reduced on the average by ~12 kJ/mol; if we increase Θ_{Ag} to 0.8, this reduction amounts to ~20 kJ/mol. An estimation of the desorption energies for the other H desorption states can again be tried on the basis of the

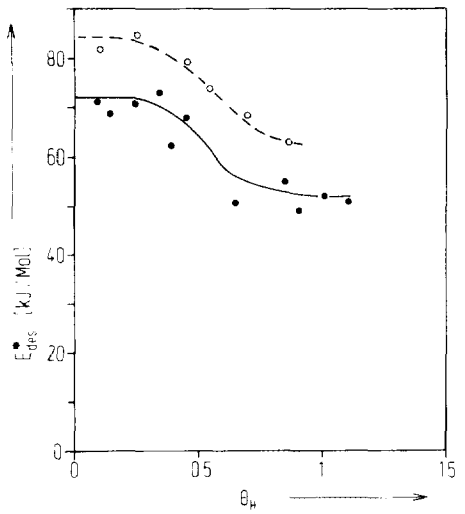

FIG. 12. Activation energy for H_2 desorption from a bimetallic Ag/Ru surface (Θ_{Ag} = 0.2, full line) as a function of H coverage, obtained from a line-shape analysis according to King (*36*). Also displayed is the corresponding function for the Ag-free, clean Ru(10$\bar{1}$0) surface (dashed line).

simple Redhead formula, cf. Eq. (1), whereby approximate 1st-order rate processes are assumed (*37*). A first-order kinetics is justified, because, as Fig. 10 shows, the TPD maxima of the β_1- and β_2- and the α-states do only slightly shift with H coverage. Apparently, the H_2 desorption from these states occurs *associatively* where the recombination of individual H atoms is no longer rate-determining. Another remarkable result is that neither the β_2-, nor the β_1- and the α-state are significantly shifted as the *silver coverage* Θ_{Ag} is increased from 0 to 0.8. Again, we obtain from a Redhead analysis (Eq. (1)) approximate desorption energies of 35 and 43 kJ/mol, for the γ_1 and γ_2-states, respectively.

Similar to the CO case, the TPD spectra and their exposure dependence allow conclusions about the adsorption kinetics of hydrogen. Although we encounter an even larger uncertainty as regards absolute numbers for Θ_H and the sticking probability s we present, in Fig. 13, a plot of the relative sticking coefficient $s' = s/s_0$ versus the hydrogen coverage for a bimetallic surface which contains Θ_{Ag} = 0.48. Note that for this Ag coverage any contribution of γ-states is not included. The remarkable result is that s' is practically constant up to a hydrogen coverage of approximately one monolayer, i.e., $\Theta_H \approx 1$, quite similar to the clean Ru(10$\bar{1}$0) case. We may interpret this finding accordingly, namely, that the H adsorption is also on the bimetallic surfaces governed by a molecular hydrogen precursor state which can, during its search for appropriate chemisorption conditions, diffuse over a fairly large surface area.

3.3.3. Work function ($\Delta\Phi$) *measurements.* Figure 14 presents an idea of how the change of the H-induced work function of bimetallic Ag/Ru surfaces is affected by the silver coverage. Figure 14a shows the exposure dependence of $\Delta\Phi$, whereas in Fig. 14b $\Delta\Phi$ is plotted against the actual H coverage (as determined from TPD). While H adsorption on clean Ru(10$\bar{1}$0) exhibits a relatively complicated exposure dependence which is characterized by a sharp initial increase to ~430 meV, a pronounced

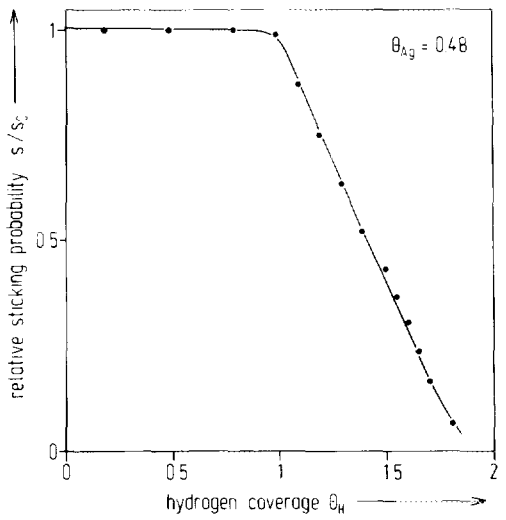

FIG. 13. Plot of the relative hydrogen sticking probability $s' = s/s_0$ against the hydrogen coverage, for a bimetallic surface containing Θ_{Ag} = 0.48; T_{ad} = 100 K. Note the practically constant sticking up to Θ_H = 1!

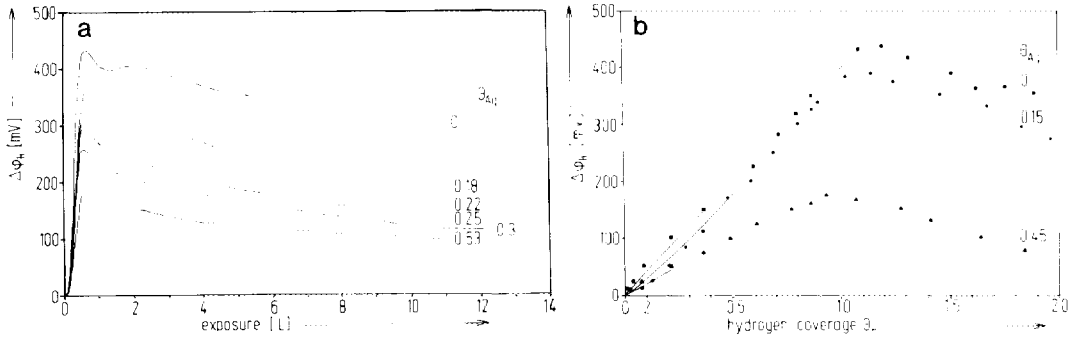

FIG. 14. (a) Exposure dependence of the H-induced work function change $\Delta\Phi$ at $T_{ad} = 100$ K, for the clean and five bimetallic Ag/Ru surfaces with Θ_{Ag} ranging from 0.18 to 0.53. (b) Hydrogen-induced $\Delta\Phi$ versus the H coverage ($T_{ad} = 100$ K), for clean Ru(10$\bar{1}$0) and two bimetallic surfaces with different silver coverages ($\Theta_{Ag} = 0.15$ and 0.45, respectively).

first maximum, a second shallower intermediate maximum of ~400 meV, and a saturation value of 350 meV (*24*), the presence of Ag results in a general decrease of $\Delta\Phi$ and a blurring of all maxima and minima; consistent with the disappearance of the sharp separation of the individual H–Ru binding states. In the $\Delta\Phi(\Theta_H)$ plot there appears only a single maximum around $\Theta_H \approx 1$. Furthermore, the initial slope $(\partial\Delta\Phi/\partial\Theta)$ decreases with increasing Ag surface concentration, pointing to a reduction of the average H-dipole moment due to silver. As in the CO case this average reduction can be either a *general* reduction of all H dipoles caused by Ag or represent a superposition of two kinds of adsorbate complexes: One unchanged (Ru-like) species with the original dipole moment μ_0 and one with a smaller charge transfer (dipole moment μ_0') which perhaps indicates H bound in Ag-like sites. From Eq. (2) we determine net dipole moments ranging from $\mu_0 = 0.12$ D for $\Theta_{Ag} = 0$ to $\mu_0 = 0.06$ for $\Theta_{Ag} = 0.45$. The γ-states, by the way, do not contribute significantly to the overall work function change, thus pointing to quite a small associated charge transfer.

4. DISCUSSION

In this discussion section we undertake the attempt to directly compare the results obtained for carbon monoxide and hydrogen adsorption on the bimetallic surfaces and to establish, if possible, a correlation between the physical properties of the bimetallic Ag/Ru system and the adsorptive behavior of our probe gases. We recall that the catalytic activity of any bimetallic system, be it an alloy or be it an inhomogeneous mixture of metals, is largely governed by both the geometrical structure and the charge distribution at the surface (= electronic structure), whereby local and long-range effects must be considered. From a more general point of view, all these phenomena can be discussed in terms of the (i) the ensemble effect, (ii) the ligand effect, and (iii) spillover activities.

4.1. The Ensemble Effect

As mentioned in the introduction, the ensemble effect deserves particular attention. Whether or not a certain ensemble is required to make CO or H adsorb on a surface consisting of an active (Ru) and an inert (Ag) species can be tackled by means of a titration technique, according to studies by Burton *et al.* (*40, 41*) and by Yu *et al.* (*42*) first performed with Au–Ni and Cu–Ni alloys, respectively. This technique is based on the validity of a linear logarithmic relationship (slope n) between the number of active ensembles (consisting of n adjacent

active atoms of kind A) and the mole fraction (surface concentration) of this active component, whereby a statistical distribution of the active and inactive (B) species is assumed. The number of ensembles is thereby taken as proportional to the total uptake of adsorbate (as determined from TPD experiments $\int p_{CO}(p_{H_2})dt$) on the respective bimetallic surface:

$$\ln\left(\int p_i dt\right) = n \cdot \ln X_A = n \cdot \ln(1 - X_B) \tag{3}$$

(A → Ru; B → Ag; i → CO or H_2 in our case). It should be noted here that this kind of ensemble size determination has been frequently used in the past and is well established (*15, 16, 40–43*); evidently, it requires the knowledge of the exact surface coverage of silver Θ_{Ag} which could, for strictly two-dimensional growth, be estimated from silver TPD data. Another problem represents the lateral distribution of the inert component on the active surface, which is, according to Section 3.1, for Ag on Ru rather island-like than statistical. In this situation Eq. (3) sets a lower limit of the ensemble size n, for the following reason: Consider a given number of inert atoms B being randomly distributed over the surface consisting of atoms of kind A. It is easily seen that this random distribution destroys the *maximum* number of ensembles A. However, if there are clusters of B, far fewer A ensembles are perturbed. Turning this argument around, it is obvious that a given decrease in the uptake of adsorbate reflects a particularly significant ensemble effect, if the diluent component is concentrated in islands (in which case only the few B atoms *not* in contact with a large B island are responsible for the overall ensemble effect). If, on the other hand, the measured decrease in the uptake refers to *all* B atoms deposited (which presumes their *statistical* distribution) the related ensemble size is minimum. In view of our ensemble size determination using Eq. (3) we have, therefore, to be aware that we obtain only a *lower limit* for n, and the actual ensemble size may be significantly larger. This uncertainty in the determination of n due to clustering of the noble metal is also well known (*44–49*). We have, in the double-logarithmic representation of Fig. 15, plotted the uptake of CO and H_2, respectively, against the "free" Ru surface concentration as determined by subtraction according to $1 - \Theta_{Ag}$. Actually, due to the smallness of the H atom, a Ru(10$\bar{1}$0) surface can accommodate *two* H atoms in the first layer, which fact must be considered when we determine H ensemble sizes in that we derive the free Ru surface concentration by subtraction of $2(1 - \Theta_{Ag})$. Figure 15a shows the results for the CO, Fig. 15b those for the H adsorption case; both times one can draw approximate straight lines whose slopes yield $n \approx 1$ for CO adsorption and $n \approx 3.7$ (→4) for dissociative hydrogen adsorption. This result, whereafter a single-site ensemble is sufficient for CO binding, but approximately a four-site ensemble for H adsorption, is in line with previous reports (*15, 43, 44*). For CO this simply means a 1 : 1 site-blocking ratio, also compatible with a terminal CO binding geometry. Our HREELS data show that no principally new adsorption site is occupied by CO; rather we presume kind of an electronic modification of those Ru sites which have one or two neighboring Ag atoms, resulting in a slight effect on both the C–O and the Ru–CO stretching frequency which is roughly proportional to the number of adjacent Ru–Ag sites. We discuss this situation in somewhat more detail in Section 4.3 (ligand effect). The observed features are different from CO adsorbed onto bimetallic Cu/Ru(0001) surfaces, where also "mixed" adsorption sites were occupied (*43*), and they differ also from recent results reported for Cu-covered Ni(111) surfaces where a new mixed Cu–Ni bridge site was found to be filled at the cost of Ni–CO top-site species (*50*).

In the H case our result means that a given ensemble of four atoms must exclusively

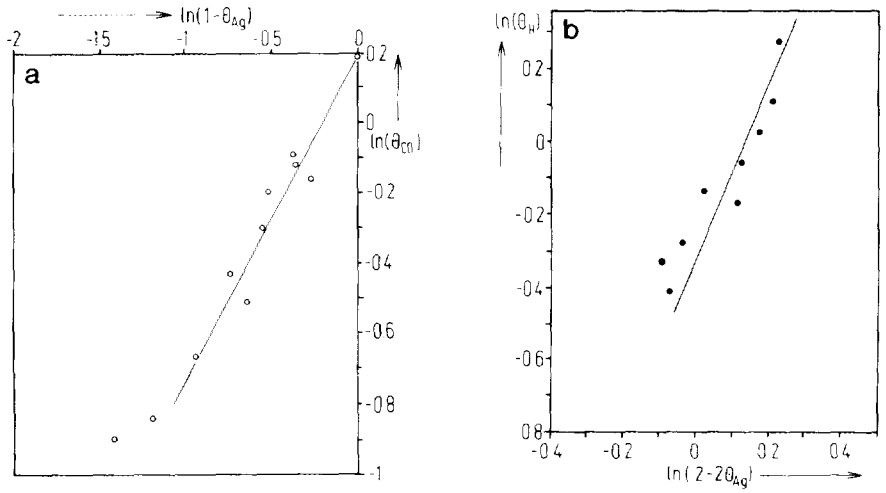

FIG. 15. Double-logarithmic plot of the adsorbed amount at saturation and the "free," that is to say *uncovered* by Ag, Ru surface area (which is assumed proportional to the surface Ru mole fraction, X_{Ru}). (a) Plot for carbon monoxide ($\Theta_{max} \approx 1$); slope ≈ 1. (b) Plot for hydrogen ($\Theta_{max} \approx 2$); slope ≈ 3.7.

consist of Ru atoms to make the hydrogen adsorb with its characteristic binding energy E_{ad}; if only a single Ag atom is mixed in, E_{ad} is so much reduced that at and above ~100 K no adsorption can take place anymore. However, it is thereby still an unresolved question whether the ensemble is necessary to *bind* H atoms sufficiently strongly, or to *dissociate* the impinging H_2 molecules. In both cases quantum-chemical arguments can be invoked: The "binding ensemble" can be explained in terms of indirect lateral interactions operating between adjacent H atoms and being conducted through the metal atoms underneath (*51, 52*). The "dissociation ensemble" may be a consequence of a dynamic gas–surface interaction and a concerted operation between the flat-lying H_2 molecule and adjacent Ru atoms forming a trapezoidal arrangement whereby the H–H intramolecular bond is transformed in a one-step process into two Ru–H bonds. Only an ensemble of a given size and geometry may provide the necessary interaction-complex geometry (*53, 54*). Note that there are also implications with regard to the kind of H–metal chemical interaction: Theories correlate the presence of an activation barrier for H_2 adsorption on noble metals and the absence of this barrier on transition metals with the role of filled or empty *d*-electron states in the dissociation process—only transition metals can provide an "escape route" to avoid Pauli repulsion and cleave the H–H bond (*55, 56*). The *binding to the surface,* however, comes about by H 1*s* interaction with the sp electrons of the metal; accordingly, the *binding-energy differences* between H–noble-metal and H–transition-metal complexes are predicted to be not very significant (*57*).

4.2. *Hydrogen Spillover*

Then, if the dissociation ensemble is the limiting factor for the H_2 uptake one could expect H *spillover* (*58*) to take place: Since there is no great difference in the adsorptive bond strength for H on a Ru-like or an Ag-like site, it could be possible for H atoms once they are formed on a Ru ensemble, to migrate to Ag sites and become adsorbed there, too. As long as there exist sufficient Ru ensembles for dissociation all Ag and Ag-like sites could become populated as well as Ru-like sites, and a rapid decrease of the hydrogen uptake $\int p_H dt$ (which is actually observed) already at small overall Ag coverages is not expected. Therefore, a spillover

effect of this kind appears less likely. On the other hand, if the binding-energy differences between Ru-like and Ag-like sites are significant, one may identify the Ag-induced γ-TPD peaks as "spillover" states which become increasingly filled only at higher H_2 exposures and sufficiently low temperatures and only, after all high-energy (Ru-like) binding sites are occupied. However, it must be assumed that despite their occupation by H atoms these sites still remain active with respect to H_2 dissociation thus providing a source of supply for H atoms to spill over to Ag-like sites. As the silver coverage increases beyond a certain limit both the size and the number of these Ru "dissociation centers" are so much reduced that this H supply is no longer sufficient to populate the γ-states. In view of our experimental observations this latter explanation seems plausible, although we cannot offer any further characterization of the *nature* of the "Ag-like" sites (for technical reasons we could not perform HREELS measurements with the H-covered Ag/Ru surfaces). We simply note that there appear *two* hydrogen γ-states which differ slightly in energy, whereby the population of the γ_1-state surpasses that of the γ_2-state considerably. The idea of H spillover is supported by recent results of Zhou *et al.* (*59*). The authors adsorbed H atoms (prepared by predissociation of H_2) on Ag(111) and found two TPD states with similar desorption temperature maxima (166 and 191 K). Of course, we are aware that we do not have any *direct* hint to hydrogen spillover, and one could interpret the γ-states with equal justification as being caused by "direct" H adsorption into Ru sites which are electronically modified by Ag atoms.

4.3. Electronic (Ligand) Effects

Electronic interaction between the two components of the bimetallic system is always to be expected, and there are indeed numerous reports in favor of this so-called ligand effect (*7, 60*). An important very recent report of Rodriguez *et al.* (*60*) dealt with the Cu/Ru bimetallic system where serious hints were presented that modified Ru adsorption sites with a strongly reduced heat of adsorption were formed. In Section 4.2 we have argued that also in the present case of Ag/Ru(10$\bar{1}$0) an alternative explanation of the CO and H γ-states (instead of spill-over) could be the formation of electronically altered Ru sites. From work function measurements with clean Ag/Ru surfaces we can indeed deduce that a partial charge transfer from Ag to the Ru surface atoms takes place (*22*), and the $\Delta\Phi$ data obtained with CO and H adsorption (altered μ_0!) could also point in this direction. Probably the most direct evidence for marked changes in the surface electronic charge distribution comes from the observation whereafter all H LEED-superstructures are suppressed even at small Ag concentrations. It is well known that any H long-range order is established by the aforementioned *indirect* lateral interactions (*51, 52*) which may be thought of as a "sharing" of binding electrons of adjacent metal atoms by a single H adsorbate atom leading to charge modifications also in the range of second and third neighbor metal atoms, sometimes even in an oscillatory manner. Mixing-in of Ag 5*s* electrons could easily perturb the overall lateral charge distribution and, hence, inhibit the long-range order characteristic of H layers on clean Ru(10$\bar{1}$0).

Any electronic (that is *chemical*) modification should in some way affect the adsorbate binding situation, that is, the adsorption energy. If we scrutinize our respective data for both CO and H, we immediately realize that up to medium Ag coverages there occurs a small but *rigid* shift particularly of the respective high energy binding state (β_3) toward lower temperatures, indicating a net reduction of the adsorptive binding energy. This Ag-induced binding-energy reduction is more pronounced for CO (~40 kJ/mol) than for H (~ 10 kJ/mol), but is in each case limited to the high-energy (β_3) state only as can be seen from Figs. 4 and 12. The fact, whereaf-

ter CO's binding energy suffers a larger downshift than that of hydrogen sheds some light on the peculiar differences between CO and H bonding to Ru: According to the Blyholder model (*39*) it is mainly the energy position and the degree of *d*-electron band filling which accounts for the CO–Ru bond strength, whereas the H chemisorption is rather dominated by sp electron states. Both our TDS and HREELS data (cf., Fig. 8b) then suggest a weakening of the OC–Me and a strengthening of the C≡O bond indicative of a slight reduction of *d*-electron state density. On the other hand, the (small) $\Delta\Phi$ decrease of Ru caused by Ag (*22*) would imply a *donation* of some charge from Ag to Ru. If we believe in the validity of the simple Blyholder model, it would follow that this extra charge reduces especially the *d*-electron state density *right at the Fermi level*, whereas other *d*-states could even become enhanced. The majority of the donated charge, however, is then expected to hybridize to Ru *sp*-like states. At this point it is, however, felt that a serious discussion of these charge effects in conjunction with thermodynamic adsorption energies and vibrational loss frequencies suffers from the lack of detailed information about surface electronic states. This can only be obtained from careful angle-resolved and polarization-dependent photoemission experiments, which have not been performed for the present system.

As another interesting point we emphasize that already at quite low Ag coverages even small amounts of adsorbate undergo the aforementioned binding energy reduction in practically the same way. This suggests that *all* adsorbed molecules or atoms are more or less affected in the same way which can only be reconciled with a *long-range* phenomenon: Not only is the adsorption energy of a Ru site reduced in the direct vicinity of silver nuclei or at the perimeters of Ag islands, but everywhere else in practically the same manner. If only those Ru atoms become energetically modified which are next to Ag then one would expect that the majority of the adparticles remains adsorbed with its characteristic energy, and only a minority should experience a net loss in adsorption energy. We cannot rule out that such an effect is superimposed on the adsorption energetics, i.e., the possibility that *in addition to* the overall energy reduction there is a special (and higher) decrease of adsorbates located directly in the vicinity of silver (the spectral resolution of our TPD spectra is such that a small amount of species with lower E^*_{des} cannot be separated from the main feature). As Θ_{Ag} increases beyond a certain limit ($\approx$0.5 . . . 0.6) there are only very few Ru atoms or ensembles left in which there are no direct Ag neighbors present; in other words, *all* sites are more or less directly modified by silver and, accordingly, we observe increasingly broadened TPD features indicating a strong energetic heterogeneity of these remaining sites. It is remarkable that the same conclusions must be drawn (at least for CO) from our vibrational loss measurements which revealed only a slight frequency shift but no evidence for a new adsorption state.

As a summary, we may state that the interaction between Ag and Ru leads to modifications of the surface electronic structure with a noticeable long-range character. Both CO and H_2 adsorption is thereby altered in a similar manner, whereby the specific CO–Ru binding is more affected than the H–Ru binding. The reverse is true, if we look at the lateral adsorbate interactions: While the CO ordering is hardly affected by Ag, there occurs a very effective suppression of H ordering.

Basically similar results have been obtained in previous reports on other bimetallic surfaces. Apparently, neither the anisotropic orientation of the Ru(10$\bar{1}$0) surface nor the formation of a well-ordered Ag layer (c(2 × 2)-structure!) seems to affect the general behavior which one can briefly characterize by a pronounced ensemble effect for H_2 adsorption and by a slight, but general, Ag-induced electronic modification of all Ru sites, resulting in an unspecific decrease of

the adsorption energy with increasing noble metal concentration.

ACKNOWLEDGMENTS

Our sincere thanks goes to Mrs. K. Schubert for drafting the figures and other technical assistance. This project was in part financed by the Deutsche Forschungsgemeinschaft (through SFB 6). One of us (P.L.) is grateful to the DFG for an "Auslandsstipendium."

REFERENCES

1. See, for example, Sinfelt, J. H. "Bimetallic Catalysis." Wiley, New York, 1983.
2. Sachtler, J. W. A., and Somorjai, G. A., *J. Catal.* **81,** (1983).
3. Ponec, V., *in* "Catalyst Characterization Science (M. L. Deviney and J. L. Gland, Eds.), ASC Symposium Series, Vol. 288, p. 267. American Chem. Soc., Washington, DC, 1985.
4. DeJongste, H. C., and Ponec, V., *J. Catal.* **63,** 389 (1980).
5. DeJongste, H. C., Ponec, V., and Gault, F. G., *J. Catal.* **63,** 395 (1980).
6. Campbell, C. T., *Annu. Rev. Phys. Chem.* **41,** 775 (1990).
7. van der Planck, P., and Sachtler, W. M. H., *J. Catal.* **7,** 300 (1967); **12,** 35 (1968).
8. Seib, D. H., and Spicer, W. E., *Phys. Rev. B* **2,** 1676 (1970).
9. Jänsch, H. J., Huang, C., Ludviksson, A., Redding, J. D., Metiu, H., and Martin, R., *Surf. Sci.* **222,** 199 (1989).
10. Konrad, B., Rieger, R., Schnell, R. D., Steinmann, W., and Wandelt, K., BESSY-Jahresbericht (hrg. Elektronenspeicherringges. m.b.H.), p. 186. Berlin, 1985.
11. Wandelt, K., Markert, K., Dolle, P., Jablonski, A., and Niemantsverdriet, J. W., *Surf. Sci.* **189,** 114 (1987).
12. Niemantsverdriet, J. W., Dolle, P., Markert, K., and Wandelt, K., *J. Vac. Sci. Technol. A* **5,** 875 (1985).
13. Park, C., *Surf. Sci.* **203,** 395 (1988).
14. Harendt, C., Sakakini, B., van den Berg, J. A., and Vickerman, J. C., *J. Electron. Spectrosc. Relat. Phenom.* **39,** 35 (1986).
15. Harendt, C., Christmann, K., and Hirschwald, W., *Surf. Sci.* **165,** 413 (1986).
16. Christmann, K., Ertl, G., and Shimizu, H., *J. Catal.* **61,** 397 (1980).
17. Brown, A., and Vickerman, J. C., *Surf. Sci.* **140,** 261 (1984).
18. Houston, J. E., Peden, C. H. F., Feibelman, P. J., and Haman, D. R., *Phys. Rev. Lett.* **56,** 375 (1986).
19. Houston, J. E., Peden, C. H. F., Blair, D. S., and Goodman, D. W., *Surf. Sci.* **167,** 427 (1986).
20. Hoffmann, F. M., and Paul, J., *J. Chem. Phys.* **84,** 2990 (1987).
21. Kiskinova, M., Tikhov, M., and Bliznakov, G., *Surf. Sci.* **204,** 35 (1988).
22. Lenz, P., and Christmann, K., in preparation.
23. Thomas, G. E., and Weinberg, W. H., *J. Chem. Phys.* **70,** 1437 (1979).
24. Lauth, G., Schwarz, E., and Christmann, K., *J. Chem. Phys.* **91,** 3729 (1989).
25. Lauth, G., Solomun, T., Hirschwald, W., and Christmann, K., *Surf. Sci.* **210,** 201 (1989).
26. Hansen, W., Bertolo, M., and Jacobi, K., *Surf. Sci.* **253,** 1 (1991).
27. Johannsson, P. K., *Surf. Sci.* **104,** 510 (1981).
28. Gregory, A. R., Gelb, A., and Silbey, R., *Surf. Sci.* **74,** 497 (1978).
29. Lindroos, M., Pfnür, H., and Menzel, D., *Surf. Sci.* **192,** 421 (1987).
30. Christmann, K., *Mol. Phys.* **66,** 1 (1989).
31. Christmann, K., and Ertl, G., *Thin Solid Films* **28,** 3 (1975).
32. Sharpio, A. P., Miller, T., and Chiang, T.-C., *Phys. Rev. B* **37,** 3996 (1988).
33. Peebles, H. C., Beck, D. D., White, J. M., and Campbell, T. C., *Surf. Sci.* **150,** 120 (1985).
34. Rhead, G. E., Barthes, M. G., and Agile, C., *Thin Solid Films* **82,** 201 (1981).
35. Kashchiev, D., *J. Cryst. Growth* **40,** 29 (1977).
36. King, D. A., *Surf. Sci.* **47,** 384 (1975).
37. Redhead, P. A., *Vacuum* **12,** 203 (1962).
38. Kisliuk, P. J., *J. Phys. Chem. Solids* **3,** 95 (1957); **5,** 78 (1958).
39. Blyholder, G., *J. Phys. Chem.* **68,** 2772 (1964).
40. Burton, J. J., and Hyman, E., *J. Catal.* **37,** 114 (1975); **37,** 1 (1975).
41. Burton, J. J., Helms, C. R., and Polizotti, R. S., *J. Chem. Phys.* **65,** 1089 (1976).
42. Yu, K. Y., Ling, D. T., and Spicer, W. E., *J. Catal.* **44,** 373 (1976).
43. Vickerman, J. C., Christmann, K., and Ertl, G., *J. Catal.* **71,** 175 (1981).
44. Vickerman, J. C., and Christmann, K., *Surf. Sci.* **120,** 1 (1982).
45. Campbell, C. T., Paffett, M. T., and Voter, A. F., *J. Vac. Sci. Technol. A* **4,** 3055 (1986).
46. Foord, J. S., and Jones, P. D., *Surf. Sci.* **152/153,** 487 (1985).
47. Peebles, H. C., Beck, D. D., White, J. M., and Campbell, C. T., *Surf. Sci.* **150,** 120 (1985).
48. Davies, P. W., Quinlen, A. M., and Somorjai, G. A., *Surf. Sci.* **121,** 290 (1982).
49. Paffett, M. T., Campbell, C. T., Taylor, T. N., and Srinivasan, S., *Surf. Sci.* **154,** 284 (1985).
50. Feng, X. H., Yu, M. R., Yang, S., Meigs, G., and Garfunkel, E., *J. Chem. Phys.* **90,** 7516 (1989).
51. Grimley, T. B., *Proc. Phys. Soc.* **90,** 751 (1967).
52. Christmann, K., *Surf. Sci. Rep.* **9,** 1 (1988).

53. Frennet, A., *in* "Hydrogen Effects in Catalysis" (Z. Paàl and G. Menon, Eds.), p. 399. Dekker, New York, 1988.
54. Christmann, K., *in* "Hydrogen Effects in Catalysis" (Z. Paàl and G. Menon, Eds.), p. 3. Dekker, New York 1988.
55. Harris, J., *Appl. Phys. A* **47,** 63 (1988).
56. Halstead, D., and Holloway, S., *J. Chem. Phys.* **93,** 2859 (1990).
57. Nørskov, J. K., and Lang, N. D., *Phys. Rev. B* **21,** 2136 (1980).
58. See, for example, "Spillover of Adsorbed Species" (G. M. Pajonk, S. J. Teichner, and J. E. Germain, Eds.). Elsevier, Amsterdam, 1983.
59. Zhou, X. L., White, J. M., and Koel, B. E., *Surf. Sci.* **218,** 201 (1989).
60. Rodriguez, J. A., Campbell, R. A., and Goodman, D. W., *J. Phys. Chem.* **95,** 2477 (1991).